

The role of the radial electric field and plasma rotation for the W7-AS stellarator confinement

J. Baldzuhn, R. Burhenn, O. Heinrich, J. Hofmann, M. Kick,
H. Maassberg, W. Ohlendorf, W7-AS Team
Max-Planck-Institut für Plasmaphysik, EURATOM-Association,
85748 Garching, Germany

Experimental principles and neoclassical calculations

In the advanced stellarator W7-AS [1], the toroidal and poloidal plasma rotation velocity is measured by charge exchange recombination spectroscopy CXRS [2] on impurity ions, mainly on Helium. For that sake, two different spectroscopic systems are available [3], the first one with observation chords in one poloidal plane, the second one with viewing lines with an angle of roughly 50 degrees to the magnetic field lines. The CX light intensity is excited in the beam of a modulated diagnostic neutral beam injector.

From the spectral CX line intensity, Doppler line broadening and line shift, the impurity density $n_{I+1}(r)$, the impurity ion temperature $T_I(r)$ and the rotation velocities V_ϕ and $V_\theta(r)$ are determined, respectively. Here, ϕ and θ are the toroidal and poloidal angle co-ordinates. The CX reaction changes the impurity charge state Z from $I+1$ to I . It is assumed that $T_I(r) = T_{I+1}(r)$. The radial electric field profile $E_r(r)$ is calculated from the simplified radial force balance equation [4]:

$$E_r = \frac{\partial(n_{I+1}(r) \cdot T_{I+1}(r))}{\partial r} \cdot \frac{1}{e Z_{I+1} n_{I+1}(r)} + \frac{T_I(r)\gamma}{e Z_I} \cdot \frac{\partial \zeta_I / \partial r}{\zeta_I} + (B_\theta V_\phi - B_\phi V_\theta) \quad (1)$$

Here, B stands for the magnetic field, e for the elementary charge, ζ_I is the excitation probability for the CX spectral line under consideration. The lifetime τ_I of the excited state and the ion gyro frequency ω_I are taken into account for the factor γ :

$$\gamma = \frac{(\omega_I \tau_I)^2}{1 + (\omega_I \tau_I)^2} \quad (2)$$

In eq. (1), the first term on the right hand side gives the impurity ion pressure gradient contribution to E_r . The second term arises from finite lifetime of the excited electronic state during the ion gyro motion after CX, for the case that the spectroscopic line of sight \vec{l} is perpendicular to the magnetic field, and a gradient of the excitation probability exists, perpendicular to \vec{l} and \vec{B} . In W7-AS this direction is parallel to the minor radius r , therefore the derivatives are with respect to r . Eq. (1) holds for CX approximately for $\gamma \ll 1$, as this is given in our case for He^+ , and therefore that second term is small. The third term is the $\vec{J} \times \vec{B}$ force. In stellarators, the toroidal and poloidal rotation are de-coupled, in contrast to tokamaks [14]. It is found experimentally for W7-AS that the main contribution to E_r comes from the poloidal rotation, the toroidal rotation is strongly damped because of

the missing axi-symmetry of the magnetic stellarator field. A fast toroidal plasma motion can be provoked only by non balanced neutral beam heating NBI, with counteracting toroidal viscosity which is found to be in good agreement to neoclassical calculations [9]. But even then its contribution to E_r is negligible (typically $< 5\%$), because $B_\theta \ll B_\phi$.

In non-axisymmetric devices like stellarators a strong dependence of transport from E_r is expected from neoclassical theory. The formation of E_r is determined by the radial particle fluxes Γ from the ambipolarity condition:

$$\Gamma_e(r, E_r) + \Gamma_i(r, E_r) + Z_1 \Gamma_1(r, E_r) = 0 \quad (3)$$

Especially in the long mean free path regime LMFP, the differences between tokamaks and stellarators are essential, because in LMFP the ripple of the magnetic field along the field lines produces large populations of trapped particles in stellarators, with different trapping types (toroidally, helically or combinations) with an enhanced radial drift. With respect to the development of a stellarator-reactor this unfavourable effect has to be minimized, as this is done by the so-called optimization concept for the advanced stellarators W7-AS and W7-X [12]. These drifts are also strongly reduced by the ambipolar E_r , an effect which is for the ions much more pronounced than for the electrons.

The neoclassical definitions for the particle fluxes Γ and heat fluxes Q are given by:

$$\begin{aligned} \Gamma_\alpha &= -n_\alpha \left\{ D_{11}^\alpha \left(\frac{n'_\alpha}{n_\alpha} - \frac{q_\alpha E_r}{T_\alpha} \right) + D_{12}^\alpha \frac{T'_\alpha}{T_\alpha} \right\} \\ Q_\alpha &= -n_\alpha T_\alpha \left\{ D_{21}^\alpha \left(\frac{n'_\alpha}{n_\alpha} - \frac{q_\alpha E_r}{T_\alpha} \right) + D_{22}^\alpha \frac{T'_\alpha}{T_\alpha} \right\} \end{aligned} \quad (4)$$

The subscript α stands for ions or electrons, respectively, q for their electric charge, D are the coefficients of the transport matrix. For the definition of Γ , a possible Ware's pinch term proportional to D_{13}^α is neglected. Besides the linear dependence of Γ and Q from E_r , also the D 's are functions of E_r , for the ions much stronger than for the electrons. For E_r , an odd number of solutions is expected from neoclassical theory [13]. Two of them should be stable, the others are unstable.

For the neoclassical calculation of E_r the numerical DKES code [5] is used. Starting from the specific magnetic configuration, represented by Fourier modes of the magnetic field, DKES calculates the mono-energetic transport coefficients by solution of the drift-kinetic equation, as function of the effective minor radius, the collisionality and E_r . By energy convolution, the 3×3 thermal transport matrix D_{ij}^α is then obtained, which is used to calculate the radial particle fluxes following eq. (4). The solution of the ambipolarity condition (3) provides then the solutions for the neoclassical E_r , which are finally compared to the measured one.

E_r and transport in W7-AS

For the case of low electron collisionality (low electron density $n_e(0)$ below $3 \cdot 10^{19} \text{ m}^{-3}$, high electron temperature $T_e(0)$ above 2 keV) only one strong positive solution is expected in W7-AS near the plasma center, the "electron root", with $E_r \approx +400 \text{ V/cm}$. For that particular case, the central electron heat transport is considerably reduced [10], allowing experimentally for maximum $T_e(0)$ up to 4 keV. This situation can be obtained only in conjunction with rather low T_i , typically below 400 eV.

For the case of higher $n_e(0)$ (between $4 - 12 \cdot 10^{19} \text{ m}^{-3}$), only one negative solution is expected near the plasma edge, the "ion-root". For that type of discharge, with combined NBI and ECRH heating and high power $> 1 \text{ MW}$, maximum negative $E_r \approx -1000 \text{ V/cm}$ are obtained in the gradient region which act as a potential barrier, together with maximum $T_i(0)$ up to 1.5 keV. The global energy confinement time exceeds the prediction from the ISS95 regression database [11] by more than a factor of two.

Multiple field solutions are expected for medium $n_e(0)$ between $2 - 5 \cdot 10^{19} \text{ m}^{-3}$ and lower heating power, typically with negative E_r values ("ion-root") near the plasma edge but smaller values than described above for $E_r \approx -100$ to -400 V/cm , and either strong positive E_r ("electron-root") near the plasma center for sufficiently high $T_e > 2 \text{ keV}$, or small positive $E_r \approx +20 \text{ V/cm}$ for lower T_e (positive "ion-root").

The comparison between the measured and calculated E_r is a sensitive means to investigate the mutual interference between E_r and the particle transport in detail [6]. It is found that the measured and the neoclassically calculated E_r are in general consistent to each other [7]. Thus, the validity of the neoclassical particle transport model for the prediction of E_r in W7-AS is demonstrated, at least for the central part of the plasma up to $r < 0.7 \cdot a$. The most striking feature appears when investigating the impact of E_r on the shape of impurity density profiles because of the higher Z. This point is of particular interest for a future stellarator reactor, because impurity accumulation has to be prevented, and efficient Helium exhaust is desired. For the calculation of the impurity density profiles, the SITAR code [8] is used which employs a tokamak axisymmetric magnetic field model. The flux ansatz $\Gamma_i = -D_i \cdot n_i' - V_i \cdot n_i$ with diffusion and convection is used in SITAR in the form:

$$\Gamma_i = \frac{\rho^2}{Z_i \tau} (0.5 + q^2) \left(B \frac{\partial n_i}{\partial r} - \frac{n_i}{Z_i n_i} \frac{\partial n_i}{\partial r} - A \frac{n_i}{T_i} \frac{\partial T_i}{\partial r} - \frac{n_i}{T_i} e Z_i E_r \right) \quad (5)$$

where ρ stands for the mean path length between two collisions, τ is a mean collision time, q is the tokamak safety factor, A and B are collisionality dependent factors [15]. SITAR fulfils internally the ambipolarity condition, thus taking into account the E_r influence implicitly. The detailed information on the stellarator magnetic field as required for the explicit calculation of the transport coefficients for W7-AS, however, is taken into account only by DKES. For some discharges, which in principle allow for multiple solutions as described above, small positive $E_r \approx +10 \text{ V/cm}$ (positive "ion-root") are predicted by DKES

in W7-AS near the plasma center. In the gradient region, the "ion-root" is negative with values $E_r \approx -100$ V/cm. The spectroscopic E_r measurement bars in this case are, however, too large to confirm the small central positive E_r from the evaluation following eq. (1) alone, see fig. 1 on the left side. The spectroscopic measurement by CXRS in fact shows a hollow He^{++} density profile for that type of discharge, as plotted in fig. 1 below on the right side (dots and broken line). With the small positive $E_r \approx +10$ V/cm taken into account in SITAR in eq. (5), the calculated He^{++} density profile also shows that hollow shape. Thus, an outward convection for He^{++} is confirmed, as a consequence of the positive E_r .

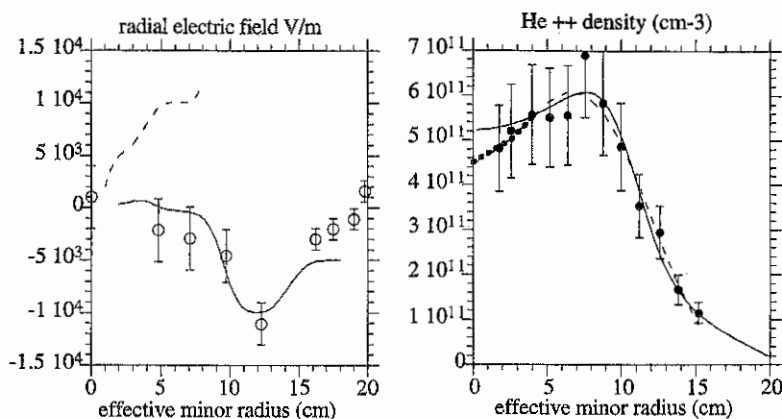


Fig. 1: Left plot: E_r profile: CXRS measurement (circles), DKES calculation for the ion-root (solid line) and the electron-root (broken line) which is not realized. The ion-root solution is positive for $r < 6$ cm. Right plot: He^{++} density profile measured by CXRS (dots), least squares fit of a generalized Gaussian function to the measured points (thin broken line), result of the SITAR transport calculation without the small positive E_r taken into account (solid line), the SITAR result with E_r reproduces the outcome of the Gaussian fit (thick dotted line).

References

- [1] Sapper J, Renner H 1990 *Fusion Technol.* **17**, 62
- [2] Fonck RJ, Darrow DS, Jaehnig KP 1984 *Phys. Rev. A* **29**, 3288
- [3] Baldzuhn J, Ohlendorf W, W7-AS Team 1997 *Rev. Sci. Instr.* **68**, 1020
- [4] Field AR, Fussmann G, Hofmann JV, ASDEX Team 1992 *Nucl. Fusion* **32**, 1191
- [5] van Rij W, Hirshman S 1989 *Phys. Fluids B* **1**, 563
- [6] Baldzuhn J et al 1995 *10th Int. Conf. Stell. Madrid EUR-CIEMAT* **30**, 144
- [7] Baldzuhn J et al, to be published
- [8] Weller A et al 1991 *Plasma Phys. Contr. Fus.* **33**, 18th EPS Conf. Berlin 1559
- [9] Hofmann JV et al 1994 *Proc. 21th EPS Conf. Montpellier*, I - 392
- [10] Brakel R, this conference; Maassberg H to be published
- [11] Stroth U et al 1996 *Nucl. Fusion* **36**, 1063
- [12] Grieger G et al 1992 *Phys. Fluids B* **4**, 2081
- [13] Mynick HE, Hitchon WNG 1983 *Nucl. Fusion* **23**, 1053
- [14] Kim YB, Diamond PH, Groebner RJ 1991 *Phys. Fluids B* **3**, 2050
- [15] Hirshman SP, Sigmar DJ 1981 *Nucl. Fusion* **21**, 1079